Journal of Engineering and Applied Sciences 11 (4): 760-766, 2016
ISSN: 1682-3915

Elasticity Solution of Functionally Graded Carbon Nanotube-Reinforced Composite Rectangular Plate

[1]Davoud Sirati, [2]Alireza Khanahmadloo, [1]Sakineh Bayat, [1]Masood Askari and [3]Amir Rajabi
[1]Department of Mechanical Engineering, Islamic Azad University, Karaj Branch, Karaj, Iran
[2]Department of Mechanical Engineering, Islamic Azad University,
Takestan Branch, Takestan, Iran
[3]Department of Mechanical Engineering, Islamic Azad University,
Savadkooh Branch, Savadkooh, Iran

Abstract: Based on three-dimensional theory of elasticity, static analysis of Functionally Graded, Carbon Nanotube Reinforced Composite (FG-CNTRC) rectangular plate subjected to mechanical load with simply supported boundary conditions is carried out. By using differential equilibrium equations and constitutive relations, state-space differential equation can be derived. The material properties of functionally graded carbon nanotube-reinforced composites are assumed to be graded through the thickness direction according to linear distributions of the volume fraction of carbon nanotubes. Detailed parametric studies have been carried out to reveal the influences of the aspect ratio, length to thickness ratio and loadings on the static behavior of plates. An accuracy of the present solutions is validated numerically by comparisons with some available results in the literature.

Key words: Static, FG, carbon nanotube, constitutive relation, thickness direction

INTRODUCTION

Modern technology demands materials having improved mechanical, thermal and chemical properties which must sustain the different environmental conditions. The Carbon Nano Tube (CNT) reinforced Functionally Graded Materials (FGM) are expected to be the new generation materials having wide range of unexplored potential applications in various technological areas such as aerospace, defense, energy, automobile, medical, structural and chemical industry. To identify the potential applications of the CNTRC structures in practice, the knowledge of the mechanical behavior of them is required. However, due to being new of this class of nanocomposites, a small proportion of research works have been done in this respect. The pure bending and bending-induced local buckling of beams reinforced by Single-Walled Carbon Nano Tubes (SWCNTs) are analyzed by (Vodenitcharova and Zhang, 2006) according to a continuum mechanical model.

Using a Mori-Tanaka approach-based continuum model (Formica *et al*., 2010) studied the vibration behavior of CNTRC plates. (Arani *et al*., 2011) employed the classical and third-order shear deformation plate theories to do the analytical and numerical investigations of buckling behavior of laminated composite plates. They determined the optimal orientation of CNTs corresponding to the maximum critical buckling load. Wu and Li (2014) have developed the finite prism method to analyze the three-dimensional free vibration of FG-CNT reinforced composite plates and laminated fiber-reinforced composite plates. Shen and Zhang (2010) have studied the thermal buckling behavior of FG-CNT reinforced composite plates subjected to in-plane temperature variation. Shen (2012) has employed the same methodology to study the thermal buckling and postbuckling behaviors of FG-CNT reinforced composite shells.

The static and free vibration characteristics of FG-CNT reinforced composite plates have been studied by Zhu *et al*. (2011) using the finite element method. Based on the Eshelby-Mori-Tanaka approach, natural frequencies characteristics of continuous FG-CNTRC cylindrical panels were studied by Sobhani *et al*. (2012). Alibeigloo (2014) has studied the static behavior of Functionally Graded Carbon Nanotube Reinforced Composite (FG-CNTRC) rectangular host plate attached to thin piezoelectric layers subjected to thermal load and or

Corresponding Author: Davoud Sirati, Department of Mechanical Engineering, Islamic Azad University, Karaj Branch, Karaj, Iran

electric field. Lei *et al.* (2013) have carried out the free vibration analysis of functionally graded carbon nanotube-reinforced composite plates using the element-free kp-Ritz method in thermal environment. The nonlinear bending of FG-CNTRC plates in thermal environment has been analyzed by Shen (2009). Eftekhari *et al.* (2013) have obtained the Ritz vibration solutions for thick skew plates. Srinivasan *et al.* (2014) have reported the vibration frequencies of skew plates by experimental and finite element methods. Wu *et al.* (2010) have studied the free vibration and buckling of highly skewed plates using the least squares finite difference method. McGee and Leissa (1991) have examined the three-dimensional free vibration behaviors of cantilevered skew plates using the Rayleigh-Ritz method. Liew *et al.* (1993) have studied the free flexural vibration of thick skew plates based on the first-order shear deformation theory using the pb-2 Rayleigh-Ritz method. Zhou *et al.* (2006) have carried out the three-dimensional vibration analysis of skew thick plates using the Chebyshev-Ritz method. Wang *et al.* (2014) have proposed a new version of the differential quadrature method to obtain a set of accurate vibration solutions of skew plates.

MATERIALS AND METHODS

Material properties of the CNTRC: FG-CNTRC plate is a mixture of the CNTs and a polymer matrix. Unlike the isotropic properties of polymer matrix, the CNTs represent anisotropic behavior. The effective material properties of this mixture can be predicted by Mori-Tanaka scheme or the rule of mixture. Based on the extended rule of mixture, the effective properties of the FG-CNTRCs can be expressed as:

$$\begin{aligned} E_{11} &= \eta_1 V_{CNT} E_{11}^{CNT} + V_m E^m \\ \frac{\eta_2}{E_{22}} &= \frac{V_{CNT}}{E_{22}^{CNT}} + \frac{V_m}{G^m} \\ \frac{\eta_3}{G_{12}} &= \frac{V_{CNT}}{G_{12}^{CNT}} + \frac{V_m}{G^m} \end{aligned} \quad (1)$$

where, E_{11}^{CNT} and E_{22}^{CNT} represent Young's moduli of the CNTs in directions 1 and 2, respectively and G_{12}^{CNT} indicates shear modulus of the CNTs. It should be noted that E_{11}, E_{22} and G_{12} are the corresponding properties of the FG-CNTRCs. In addition, E^m and G^m represent Young's modulus and shear modulus of the isotropic polymer matrix. Due to presence of small scale effect, the CNT efficiency parameters, η_i (i = 1-3) are introduced in Eq. 1. To calculate the value of the CNT efficiency parameters, elastic modulus of the FGCNTRCs predicted by the MD simulations should be matched with those determined from the rule of mixture. Moreover, V_{CNT} and V_m are the volume fractions of the CNTs and matrix, respectively and relation among these volume fractions is:

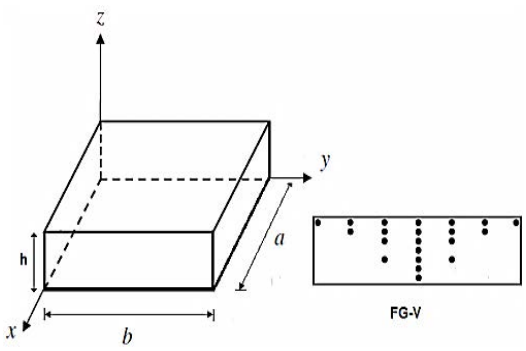

Fig. 1: Coordinate system of a FG-CNTRC plate

$$V_{CNT} + V_m = 1 \quad (2)$$

Similarly, mass density of the FG-CNTRC plates can be expressed as a function of densities of the CNTs and matrix as follows:

$$\rho = V_{CNT}\rho^{CNT} + V_m\rho^m \quad (3)$$

where, ρ^{CNT} and ρ^m indicate the densities of CNTs and matrix. In addition, Poisson's ratio can be obtained as:

$$v_{12} = V^*_{CNT} v_{12}^{CNT} + (1-V^*_{CNT})v^m \quad (4)$$

where in v_{12}^{CNT} and v^m are Poisson's ratios of the CNTs and polymer matrix, respectively and V* is defined as follow:

$$V^*_{CNT} = \frac{w_{CNT}}{w_{CNT} + (\rho^{CNT}/\rho_m)(1-w_{CNT})} \quad (5)$$

In which w_{CNT} is the mass fraction of the CNTs. Consider a FG-CNTRC plate of length a in the x direction, width b in the y direction and thickness h in the z direction. CNTs can be distributed functionally graded in the thickness of the FG-CNTRC plates as shown in Fig. 1.

Here, linear variation of volume fraction of CNT (V_{CNT}) is considered. It is calculated by following equation:

$$V_{CNT}(z) = (1 + \frac{2z}{h})V^*_{CNT} \quad (6)$$

In this present investigation, the CNT efficiency parameters η_i n relation to the given volume fraction (V^*_{CNT}) are: = $\eta_1 = 0.149$ and $\eta_2 = \eta_3 = 0.934$ for the case of $V^*_{CNT} = 0.11$.

Basic equations: Constitutive equations for rectangular plate is:

$$\begin{bmatrix}\sigma_x\\ \sigma_y\\ \sigma_z\\ \tau_{xz}\\ \tau_{yz}\\ \tau_{xy}\end{bmatrix} = \begin{bmatrix}C_{11} & C_{12} & C_{13} & 0 & 0 & 0\\ C_{21} & C_{22} & C_{23} & 0 & 0 & 0\\ C_{31} & C_{32} & C_{33} & 0 & 0 & 0\\ 0 & 0 & 0 & C_{44} & 0 & 0\\ 0 & 0 & 0 & 0 & C_{55} & 0\\ 0 & 0 & 0 & 0 & 0 & C_{66}\end{bmatrix}\begin{bmatrix}\varepsilon_x\\ \varepsilon_y\\ \varepsilon_z\\ \gamma_{xz}\\ \gamma_{yz}\\ \gamma_{xy}\end{bmatrix} \quad (7)$$

Here, C_{ij} are related to the lame constants as follow:

$$\begin{aligned} &C_{11} = \frac{E_{11}}{\Delta}(1 - v_{23}\, v_{32}), C_{22} = \frac{E_{22}}{\Delta}(1 - v_{31}\, v_{13}),\\ &C_{33} = \frac{E_{33}}{\Delta}(1 - v_{12}\, v_{21}), C_{12} = \frac{E_{11}}{\Delta}(v_{21} - v_{31}\, v_{23})\\ &C_{13} = \frac{E_{11}}{\Delta}(v_{31} - v_{21}\, v_{32}), C_{23} = \frac{E_{22}}{\Delta}(v_{32} - v_{12}\, v_{31})\\ &C_{44} = G_{23}, C_{55} = G_{13}, C_{66} = G_{12}\end{aligned} \quad (8)$$

Where:

$$\Delta = 1 - v_{12}\, v_{21} - v_{23}\, v_{32} - v_{31}\, v_{13} - 2v_{12}\, v_{32}\, v_{13}$$

And:

$$\begin{aligned} &v_{13} = v_{12}, v_{31} = v_{13}, v_{32} = v_{23} = v_{21},\\ &v_{21} = (v_{12}\, E_{22})/E_{11}\end{aligned}$$

Linear strain-displacements relations are:

$$\begin{aligned} &\varepsilon_x = \frac{\partial u}{\partial x}, \varepsilon_y = \frac{\partial v}{\partial y}, \varepsilon_z = \frac{\partial w}{\partial z}, \gamma_{xy} = \frac{\partial u}{\partial y} + \frac{\partial v}{\partial x},\\ &\gamma_{xz} = \frac{\partial u}{\partial z} + \frac{\partial w}{\partial x}, \gamma_{yz} = \frac{\partial w}{\partial y} + \frac{\partial v}{\partial z},\end{aligned} \quad (9)$$

In the absence of body forces, governing equations of motion are:

$$\frac{\partial \sigma_x}{\partial x} + \frac{\partial \tau_{xy}}{\partial y} + \frac{\partial \tau_{xz}}{\partial z} = 0 \quad (10)$$

$$\frac{\partial \tau_{xy}}{\partial x} + \frac{\partial \sigma_y}{\partial y} + \frac{\partial \tau_{yz}}{\partial z} = 0 \quad (11)$$

$$\frac{\partial \tau_{xz}}{\partial x} + \frac{\partial \tau_{yz}}{\partial y} + \frac{\partial \sigma_z}{\partial z} = 0 \quad (12)$$

State-space equations can be derived from Eq. 7-10 as the follow:

$$\frac{\partial \sigma_z}{\partial z} = -\frac{\partial \tau_{xz}}{\partial x} - \frac{\partial \tau_{yz}}{\partial y} \quad (13)$$

$$\frac{\partial u}{\partial z} = \frac{1}{C_{44}}\tau_{xz} - \frac{\partial w}{\partial x} \quad (14)$$

$$\frac{\partial v}{\partial z} = \frac{1}{C_{55}}\tau_{yz} - \frac{\partial w}{\partial y} \quad (15)$$

$$\frac{\partial w}{\partial z} = \frac{1}{C_{33}}\sigma_z - \frac{C_{13}}{C_{33}}\frac{\partial u}{\partial x} - \frac{C_{23}}{C_{33}}\frac{\partial v}{\partial y} \quad (16)$$

$$\begin{aligned} \frac{\partial \tau_{xz}}{\partial z} = &-\left(\frac{C_{11}C_{33} - C_{13}C_{13}}{C_{33}}\right)\frac{\partial^2 u}{\partial x^2} -\\ &\left(\frac{C_{12}C_{33} - C_{13}C_{13}}{C_{33}}\right)\frac{\partial^2 v}{\partial x \partial v} - \frac{C_{13}}{C_{13}}\frac{\partial \sigma_z}{\partial x} -\\ &C_{66}\frac{\partial^2 u}{\partial y^2} - C_{66}\frac{\partial^2 u}{\partial x \partial y}\end{aligned} \quad (17)$$

$$\begin{aligned} \frac{\partial \tau_{yz}}{\partial z} = &-\left(\frac{C_{12}C_{32} - C_{23}C_{13}}{C_{33}}\right)\frac{\partial^2 u}{\partial x \partial y} -\\ &\left(\frac{C_{33}C_{22} - C_{23}C_{23}}{C_{33}}\right)\frac{\partial^2 v}{\partial y^2} - \frac{C_{23}}{C_{33}}\frac{\partial \sigma_z}{\partial y} -\\ &C_{66}\frac{\partial^2 u}{\partial x \partial y} - C_{66}\frac{\partial^2 v}{\partial x^2}\end{aligned} \quad (18)$$

Equation 19 can be written in the matrix form:

$$\frac{\partial \delta}{\partial z} = G\delta \quad (19)$$

where, $\delta = [\sigma_z\, u\, v\, w\, \tau_{xz}\, \tau_{yz}]$ is column matrix of state variables and G is coefficients matrix. The relations for simply supported edges boundary conditions are:

$$x = 0, a \rightarrow \begin{cases} v(0,y) = w(0,y) = 0\\ v(a,y) = w(a,y) = 0\end{cases} \quad (20)$$

$$y = a, b \rightarrow \begin{cases} u(x,0) = w(x,0) = 0\\ u(x,b) = w(x,b) = 0\end{cases} \quad (21)$$

Solution procedure: In order to satisfy the simply supported boundary conditions, Eq. 12, displacement and stress components are assumed as:

$$\sigma_x = \sigma_x^* \sin(P_m x)\sin(P_n y), \sigma_y = \sigma_y^* \sin(P_m x)\sin(P_n y)$$
$$\sigma_z = \sigma_z^* \sin(P_m x)\sin(P_n y), \tau_{xz} = \tau_{xz}^* \cos(P_m x)\sin(P_n y)$$
$$\tau_{yz} = \tau_{yz}^* \sin(P_m x)\cos(P_n y), u = u^* \cos(P_m x)\sin(P_n y)$$
$$v = v^* \sin(P_m x)\cos(P_n y), w = w^* \sin(P_m x)\sin(P_n y) \quad (22)$$

Where:

$$P_n = \frac{n\pi}{b}, P_m = \frac{m\pi}{a}$$

The general solution for Eq. 23 can be explicitly expressed as:

$$\delta(z) = \delta_0 e^{\int_{z_0}^{z} G\,dz} \quad (23)$$

where, δ_0 and z_0 are values of δ and z at the bottom surface of plate, respectively. Equation 24 at z = h yields:

$$\delta_h = M\delta_0 \quad (24)$$

Where:

$$M = e^{\int_0^h G\,dz} \quad (25)$$

For the bending analysis, following relations for surface boundary conditions at the top and bottom surface of plate are assumed:

$$\sigma_z = -P, \quad \tau_{xz} = \tau_{yz} = 0 \text{ at } z = h$$
$$\sigma_z = 0, \quad \tau_{xz} = 0, \tau_{yz} = 0 \text{ at } z = 0 \quad (26)$$

Applying surfaces tractions, Eq. 25-26 displacement components at the bottom surface of the plate are obtained:

$$\begin{bmatrix} -P \\ 0 \\ 0 \end{bmatrix} = \begin{bmatrix} m_{12} & m_{13} & m_{14} \\ m_{52} & m_{53} & m_{54} \\ m_{62} & m_{63} & m_{64} \end{bmatrix} \begin{bmatrix} u \\ v \\ w \end{bmatrix} \quad (27)$$

By using Eq. 26, 27 and 23 state variables in three dimensions can be derived.

RESULTS AND DISCUSSION

In this investigation, polymer is used as the matrix in which material properties are:

$$u^m = 0.34, \ \rho^m = 1150 \frac{kg}{m^3}, E^m = 2.1 Gpa \quad (28)$$

For the material used to reinforce the polymeric matrix in CNTRC plates, the armchair (10, 10) SWCNTs are chosen for this purpose whose properties are:

$$u_{12}^{CNT} = 0.175, \rho^{CNT} = 1400 \frac{kg}{m^3}, E_{11}^{CNT} = 5.6466 Tpa,$$
$$E_{22}^{CNT} = 7.08 Tpa, G_{12}^{CNT} = G_{13}^{CNT} = G_{23}^{CNT} = 1.9445 Tpa \quad (29)$$

Equation 30 shows that:

$$G = \begin{bmatrix} S_{11} & S_{12} & S_{13} & S_{14} & S_{15} & S_{16} \\ S_{21} & S_{22} & S_{23} & S_{24} & S_{25} & S_{26} \\ S_{31} & S_{32} & S_{33} & S_{34} & S_{35} & S_{36} \\ S_{41} & S_{42} & S_{43} & S_{44} & S_{45} & S_{46} \\ S_{51} & S_{52} & S_{53} & S_{54} & S_{55} & S_{56} \\ S_{61} & S_{62} & S_{63} & S_{64} & S_{65} & S_{66} \end{bmatrix}$$
$$S_{11} = 0, S_{12} = 0, S_{13} = 0, S_{14} = 0$$
$$S_{15} = \frac{P_m}{\lambda}, S_{16} = \frac{P_n}{\lambda}, S_{21} = 0, S_{22} = 0$$
$$S_{23} = 0, S_{24} = -1, S_{25} = \frac{1}{C_{44}}$$
$$S_{26} = 0, S_{31} = 0, S_{23} = 0, S_{33} = 0$$
$$S_{34} = -1, S_{35} = 0, S_{36} = \frac{1}{C_{55}}$$
$$S_{41} = \frac{1}{C_{33}}, S_{42} = \frac{C_{13}}{C_{33}}, S_{43} = \frac{C_{23}}{C_{33}} P_n, S_{44} = 0$$
$$S_{45} = 0, S_{46} = 0, S_{51} = -\frac{C_{13}}{\lambda C_{33}} P_m$$
$$S_{52} = \left(\frac{C_{11} C_{33} - C_{13} C_{13}}{\lambda C_{33}} \right) P_m^2 + \frac{C_{66}}{\lambda} P_n^2$$
$$S_{53} = \left(\frac{C_{12} C_{33} - C_{13} C_{23}}{\lambda C_{33}} \right) P_m P_n + \frac{C_{66}}{\lambda} P_n P_m$$
$$S_{54} = 0, S_{55} = 0, S_{56} = 0, S_{61} = -\frac{C_{23}}{\lambda C_{33}} P_n$$
$$S_{62} = \left(\frac{C_{21} C_{33} - C_{23} C_{13}}{\lambda C_{33}} \right) P_n P_m + \frac{C_{66}}{\lambda} P_n P_m$$
$$S_{63} = \left(\frac{C_{33} C_{22} - C_{23} C_{23}}{\lambda C_{33}} \right) P_n^2, \ S_{64} = S_{65} = S_{66} = 0 \quad (30)$$

To validate the accuracy of the present approach, numerical results are extracted and tabulated in Table 1. From comparison of dimensionless transverse displacement at mid length of simply supported edges square plate with the results of (Casttellazi *et al*., 2013) presented in Table 1, good agreement can be observed.

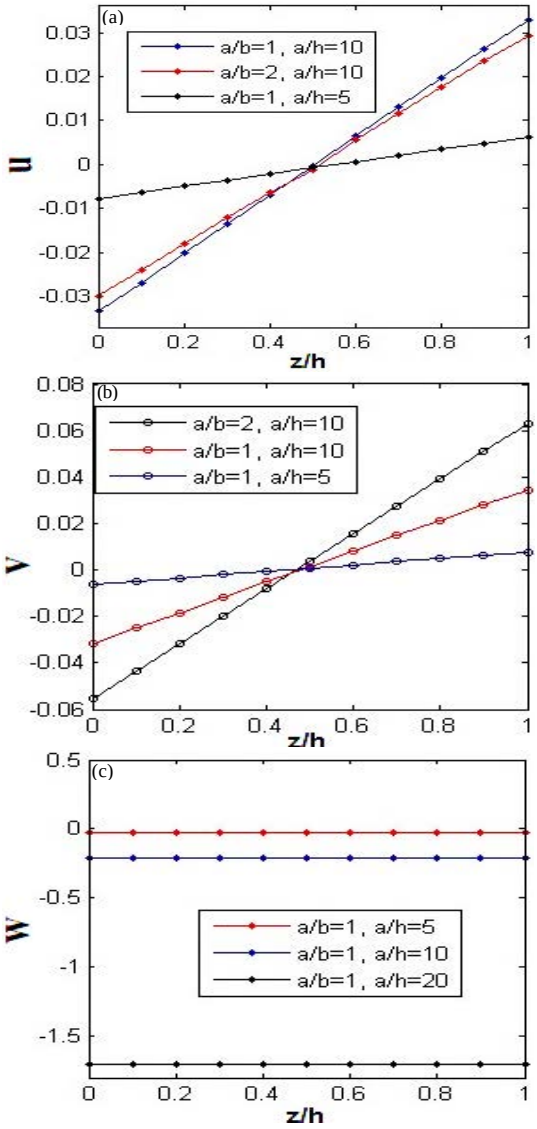

Fig. 2: The effect of aspect ratio and length to thickness ratio on the displacements (u, v, w) of rectangular FG-CNTRC plate

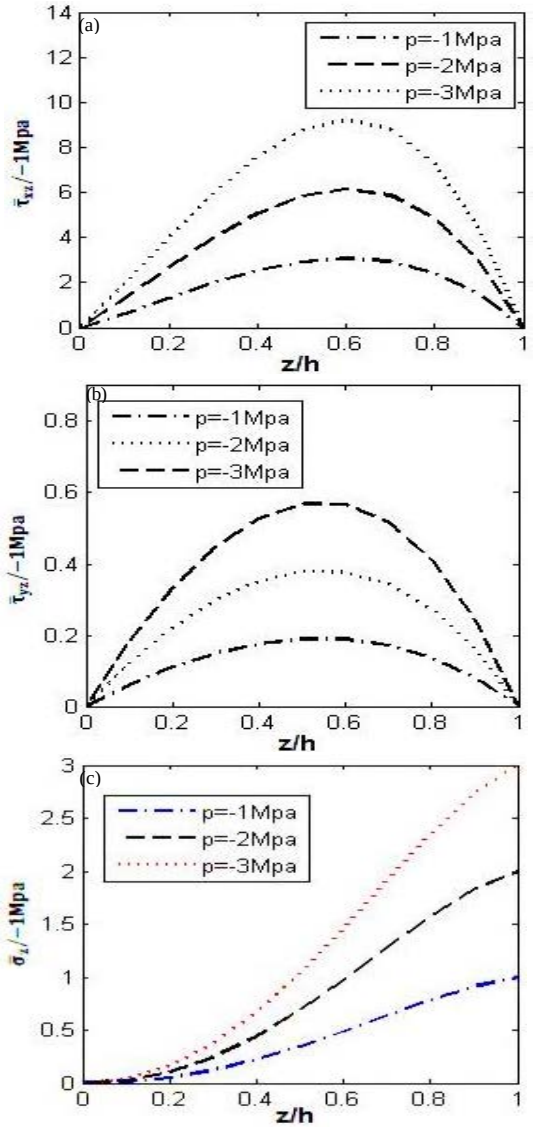

Fig. 3: The effect of load values on the stresses of rectangular FG-CNTRC plate

Table 1: Comparison of the dimensionless transverse displacement (w) at center of FG plate with simply supported edges and L/h = 10

n	Present	Ref. (Castellazzi *et al*., 2013)
0.5	0.2184	0.2176
1	0.2565	0.2473

Through the thickness distribution of displacements are depicted in Fig. 2. According to Figures, increase the length to thickness ratio causes to increase displacement of rectangular FG-CNTRC plate.

To illustrate the effect of load values on the static response of FG-CNTRC plates, shear stresses τ_{xz}, τ_{yz} and transverse stress σ_z are plotted in Fig. 3. It can be observed form Fig. 3, stresses increases with the increase of load values. Through the thickness distribution of displacements are depicted in Fig. 4. According to Figures, increase the load values causes to increase displacement of rectangular FG-CNTRC square plate.

The effect of aspect ratio on the static response of FG-CNTRC plates, shear stresses τ_{xz}, τ_{yz} and transverse stress σ_z are plotted in Fig. 5. It can be observed form Fig. 5, stresses increases with the increase of aspect ratio. Also, It can be observed form Fig. 5 shear stress τ_{yz} decreases with the increase of aspect ratio.

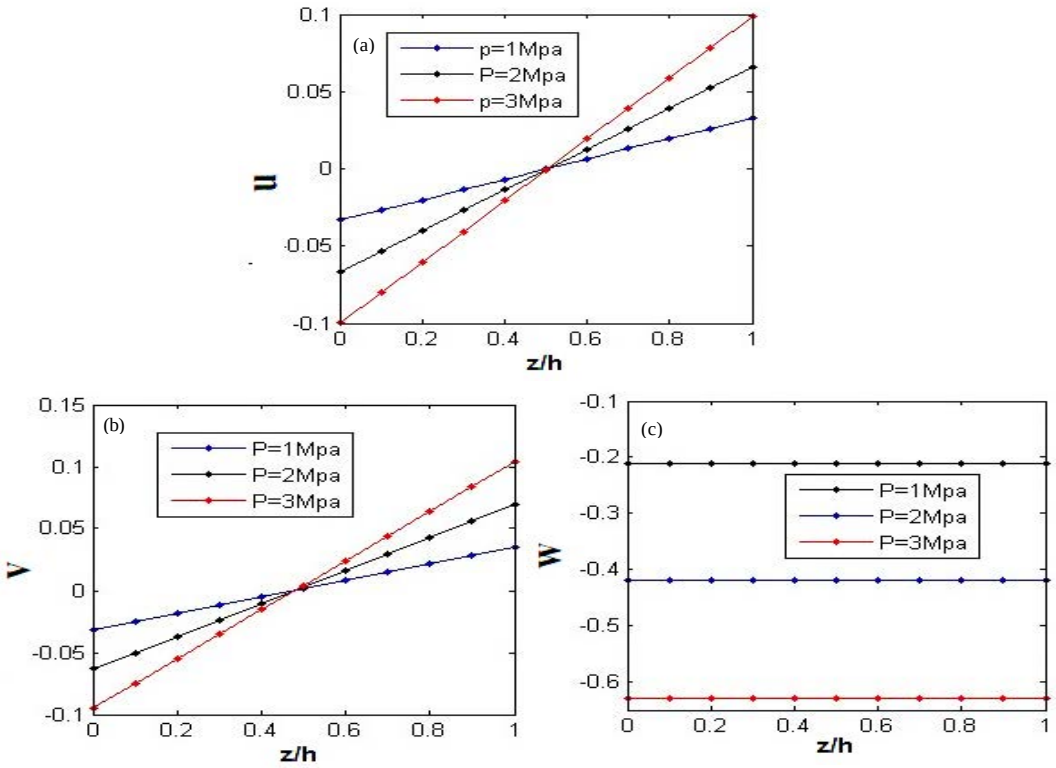

Fig. 4: The effect of load values on the displacements (u, v, w) of rectangular FG-CNTRC plate

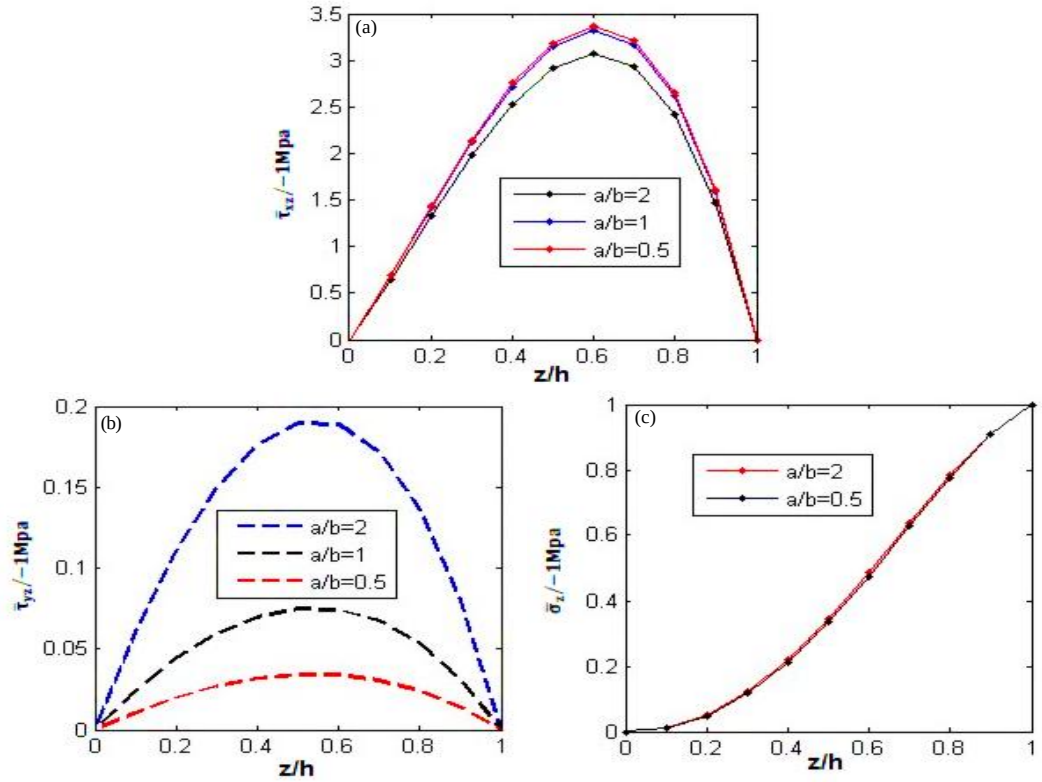

Fig. 5: The effect of aspect ratio on the stresses of rectangular FG-CNTRC plate

CONCLUSION

In this study, static analysis of Functionally Graded Carbon Nanotube Reinforced Composite (FG-CNTRC) rectangular plate subjected to mechanical load with simply supported boundary conditions is carried out using three-dimensional theory of elasticity. By using differential equilibrium equations and constitutive relations, state-space differential equation can be derived. The material properties of functionally graded carbon nanotube-reinforced composites are assumed to be graded through the thickness direction according to linear distributions of the volume fraction of carbon nanotubes. Detailed parametric studies have been carried out to reveal the influences of the aspect ratio, length to thickness ratio and loadings on the static behavior of plates. An accuracy of the present solutions is validated numerically by comparisons with some available results in the literature. Increase the load values causes to increase displacement of rectangular FG-CNTRC square plate. Increase the length to thickness ratio causes to increase displacement of rectangular FG-CNTRC plate. Increase the load values causes to increase stresses of rectangular FG-CNTRC square plate.

REFERENCES

Alibeigloo, A., 2014. Three-dimensional thermoelasticity solution of functionally graded carbon nanotube reinforced composite plate embedded in piezoelectric sensor and actuator layers. Comp. Struct., 118: 482-495.

Arani, A.G., S. Maghamikia, M. Mohammadimehr and A. Arefmanesh, 2011. Buckling analysis of laminated composite rectangular plates reinforced by SWCNTs using analytical and finite element methods. J. Mech. Sci. Technol., 25: 809-820.

Castellazzi, G., C. Gentilini, P. Krysl and I. Elishakoff, 2013. Static analysis of functionally graded plates using a nodal integrated finite element approach. Comp. Struct., 103: 197-200.

Eftekhari, S.A. and A.A. Jafari, 2013. A simple and accurate Ritz formulation for free vibration of thick rectangular and skew plates with general boundary conditions. Acta Mech., 224: 193-209.

Formica, G., W. Lacarbonara and R. Alessi, 2010. Vibrations of carbon nanotube-reinforced composites. J. Sound Vibration, 329: 1875-1889.

Lei, Z.X., K.M. Liew and J.L. Yu, 2013. Free vibration analysis of functionally graded carbon nanotube-reinforced composite plates using the element-free kp-Ritz method in thermal environment. Comp. Struct., 106: 128-138.

Liew, K.M., Y. Xiang, S. Kitipornchai and C.M. Wang, 1993. Vibration of thick skew plates based on mindlin shear deformation plate theory. J. Sound Vibration, 168: 39-69.

McGee, O.G. and A.W. Leissa, 1991. Three-dimensional free vibrations of thick skewed cantilevered plates. J. Sound Vibration, 144: 305-322.

Shen, H.S. and C.L. Zhang, 2010. Thermal buckling and postbuckling behavior of functionally graded carbon nanotube-reinforced composite plates. Mater. Design, 31: 3403-3411.

Shen, H.S., 2009. Nonlinear bending of functionallygraded carbon nanotube-reinforced composite plates in thermal environments. Comp. Struct., 91: 9-19.

Shen, H.S., 2012. Thermal buckling and postbuckling behavior of functionally graded carbon nanotube-reinforced composite cylindrical shells. Comp. Part B: Eng., 43: 1030-1038.

Srinivasa, C.V., Y.J. Suresh and W.P.P. Kumar, 2014.Experimental and finite element studies on free vibration of cylindrical skew panels. Int. J. Adv. Struct. Eng., 6: 1-11.

Vodenitcharova, T. and L.C. Zhang, 2006. Bending and local buckling of a nanocomposite beam reinforced by a single-walled carbon nanotube. Int. J. Solids Struct., 43: 3006-3024.

Wang, X., Y. Wang and Z. Yuan, 2014. Accurate vibration analysis of skew plates by the new version of the differential quadrature method. Applied Math. Mod., 38: 926-937.

Wu, C.P. and H.Y. Li, 2014. Three-dimensional free vibration analysis of functionally graded carbon nanotube-reinforced composite plates with various boundary conditions. J. Vibration Control, 22: 89-107.

Wu, W.X., C. Shu, C.M. Wang and Y. Xiang, 2010. Free vibration and buckling analysis of highly skewed plates by least squares-based finite difference method. Int. J. Struct. Stability Dynam., 10: 225-252.

Zhou, D., S.H. Lo, F.T.K. Au, Y.K. Cheung and W.Q. Liu, 2006. 3-D vibration analysis of skew thick plates using Chebyshev-Ritz method. Int. J. Mech. Sci., 48: 1481-1493.

Zhu, P. and K.M. Liew, 2011. Free vibration analysis of moderately thick functionally graded plates by local Kriging meshless method. Comp. Struct., 93: 2925-2944.